# Properties of Stream Interactions at 1 AU over the Solar Cycle: Anticipating STEREO

L. Jian[1], C. T. Russell[1], and J. G. Luhmann[2]

[1]IGPP and ESS, UC_Los Angeles, [2]Space Sciences Laboratory, UC_Berkeley

## Abstract

A Stream Interaction Region (SIR) is formed when a fast solar stream overtakes a slow stream. The signatures of SIRs evolve as they move away from the Sun. Based on the study of the Wind (1995-2004) and ACE (1998-2004) data, we find that the occurrence rate of shocks at SIRs is about 26% on average, which is unexpectedly high at 1 AU, and 16% of SIRs are associated with forward shocks. The number of SIR events varies little over the solar cycle. In order to address the effect of SIRs on geomagnetic activity, we also determine the solar cycle variation of the change in velocity from slow stream to fast stream, and the solar cycle variation of the maximum magnetic field as well as the peak total perpendicular pressure. Finally, we find that rotations of magnetic fields often occur at the sector boundary ahead of the SIR, that the north-south component of the magnetic field is typically highly fluctuating within the SIRs, and that the durations of the interaction region is quite variable.

## Introduction

The magnetic structure of the corona controls solar wind velocity. For much of the solar cycle the magnetic field in the corona, well above the photosphere, is roughly that of a dipole tilted with respect to the rotation axis of the Sun. As the solar magnetic field evolves through the 11-year solar activity cycle, this tilt varies, producing the change in the configuration of heliospheric current sheet. The dipole tends to be nearly aligned with the solar rotation axis near solar activity minimum, whereas it tends to be inclined substantially relative to the rotation axis on the declining phase of the solar cycle. Near solar activity maximum the solar magnetic field is sufficiently complex that the dipole concept is not useful.

The fast solar wind originates principally from high heliolatitudinal coronal holes, while the slow solar wind arises near the heliospheric current sheet. Since these radially aligned parcels of plasma originate from different positions on the Sun at different times, they are threaded by different magnetic field lines and are thus prevented from interpenetrating. When they move away from the Sun, the faster wind runs into slower wind ahead while simultaneously outrunning slower trailing wind as indicated in Figure 1. A compression forms on the rising-speed portion of a high-speed stream and a rarefaction forms on the trailing edge. Because the pattern of compression rotates with the Sun when the outflow from the Sun is time stationary, these high pressure regions are often called Corotating Interaction Regions (CIRs). Here, we use the name, Stream Interaction Regions (SIRs), to include some transient and local stream interactions, which do not last even one rotation, and hence can not be considered to be corotating.

The interaction between fast and slow solar wind begins in the inner heliosphere, SIRs thus are commonly well formed at Earth's orbit, 1AU from the Sun. The stream interfaces are distinguished as abrupt drops in particle density with simultaneous rises in proton temperature, and a large shear in the flow within SIRs. As the SIRs move farther away from the Sun, they eventually coalesce.

Magnetic field does not exert pressure along its length, but the magnetic field and plasma both contribute to the perpendicular pressure force. Since the dynamics of the solar wind structures is controlled by the total perpendicular pressure Ptpp, $B^2/2\mu_0+nkT$, and not by the constituents individually, we obtain simpler signatures in Ptpp than in the signatures of the constituent components. Moreover, irregularities in Ptpp are smoothed by compressional waves that radiate away inhomogeneities in pressure, leaving only sudden discontinuities caused by shocks. The peak pressure is equal to the dynamic pressure of the flow on either side of the stream interface resolved along the normal to the boundary and in the reference frame of the boundary. Shocks arise when the change in velocity across the plasma interface exceeds the compressional wave speed so that linear waves can not act to transmit the pressure from the interaction into the surrounding plasma. At forward shocks, solar wind speed increases, while simultaneously proton number density and temperature both increase. At reverse shocks, solar wind speed again increases, while proton number density and temperature both decline.

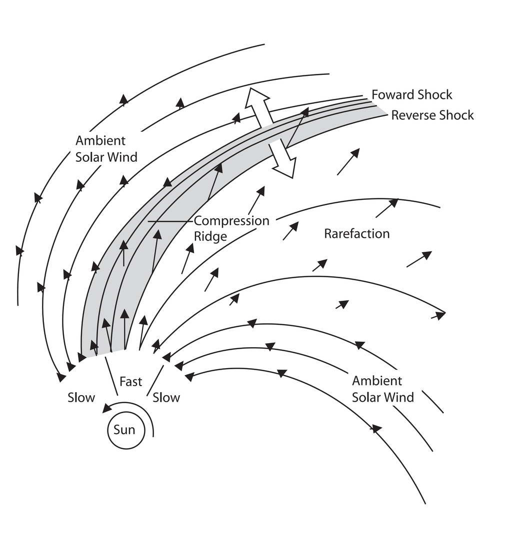


**Figure 1.** Schematic illustrating 2-D corotating stream structure in the solar equatorial plane in the inner heliosphere (after Pizzo, 1978)

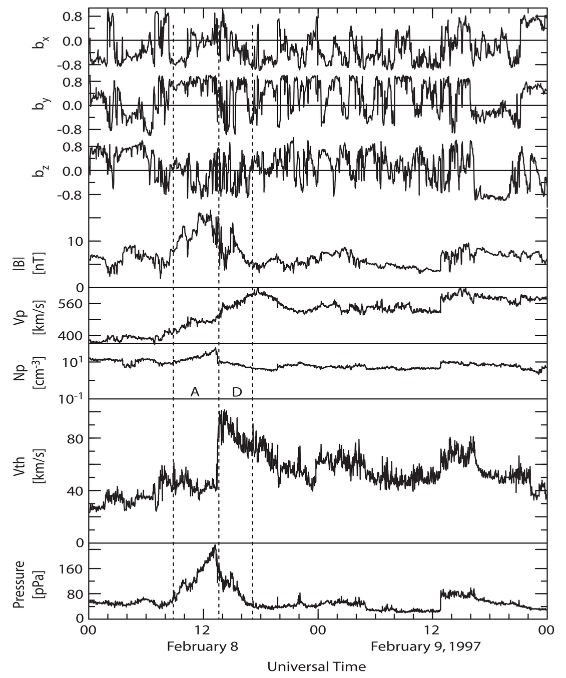


**Figure 2.** SIR Event 1 without shocks.

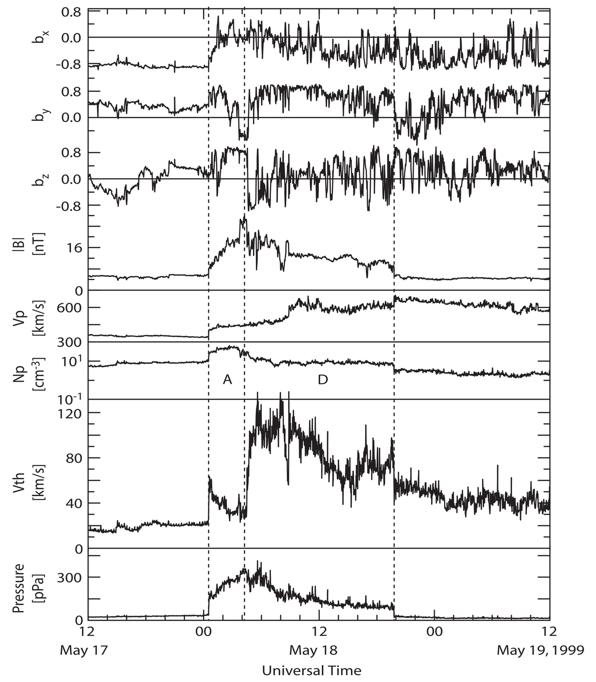


**Figure 3.** SIR Event with forward-reverse shocks.

**Figure 5.** Annual Statistics of Some Properties of SIRs

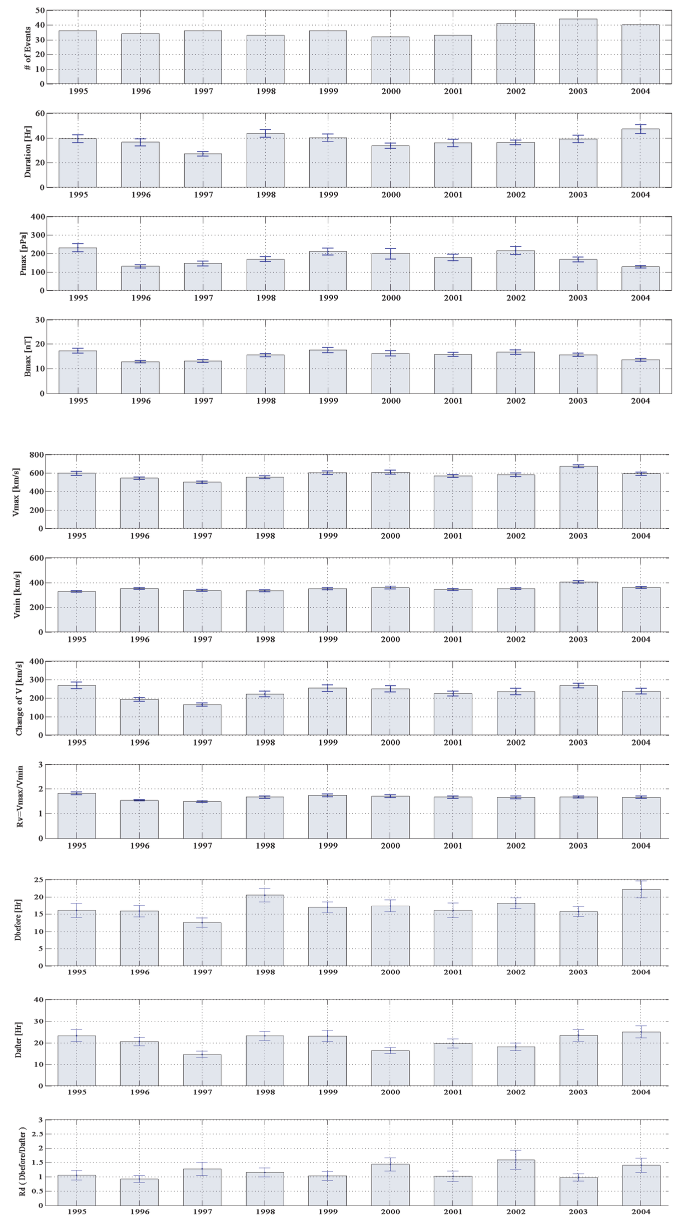

**Figure 6.** Annual Statistics of Some Properties of CIRs

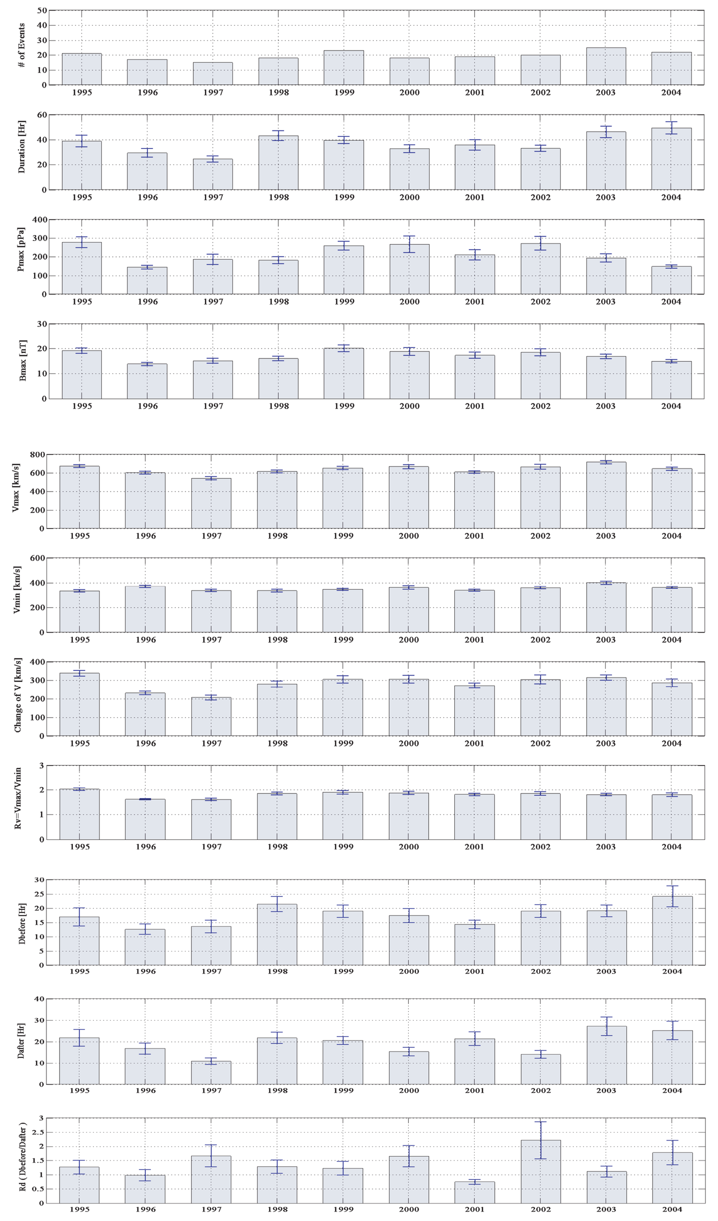

**Table 1. A Sample of the List of SIRs and CIRs**

| SIR # | CIR # | Start UT | End UT | Duration [Hr] | Discontinuity UT | F/R Shock | ΔP [pPa] | | Stream Interface UT | Pmax [pPa] | Vmax [km/s] | Vmin [km/s] | ΔV [km/s] | Bmax (nT) | Comments |
|---|---|---|---|---|---|---|---|---|---|---|---|---|---|---|---|
| | | | | | | | 1998 | | | | | | | | |
| 1 | | 01/16 0900 | 01/17 1200 | 27.00 | | | | | 01/16 1804 | 130 | 380 | 280 | 100 | 14 | good example of SIR, not CIR |
| 2 | | 01/18 0600 | 01/20 2000 | 62.00 | | | | | 01/19 1400 | 180 | 470 | 290 | 180 | 17.8 | |
| 3 | | 01/31 1400 | 02/01 1500 | 25.00 | 01/31 1553 | F | 60 -> 150 | 90 | 01/31 2345 | 170 | 480 | 330 | 150 | 14.5 | V irregular, noisy, cataching up an ICME |
| 4 | | 02/10 1800 | 02/11 2300 | 29.00 | | | | | 02/11 1520 | 80 | 580 | 390 | 190 | 10.3 | |
| 5 | | 02/28 0000 | 03/03 0000 | 72.00 | | | | | 02/28 1415 | 150 | 515 | 310 | 205 | 15 | P peaks not where T sharply rises |
| 6 | 1 | 03/09 2100 | 03/11 0400 | 55.00 | | | | | 03/10 1015 | 300 | 565 | 270 | 295 | 23.5 | noisy, trough in the center |
| 7 | 2 | 03/19 2000 | 03/22 1200 | 64.00 | | | | | 03/21 1100 | 160 | 640 | 310 | 330 | 16 | 3 peaks of P |
| 8 * | | 03/24 1000 | 03/27 2300 | 85.00 | | | | | 03/26 0256 | 100 | 510 | 350 | 160 | 13 | containing a flux rope structure |
| 9 | | 04/03 2200 | 04/05 0600 | 32.00 | | | | | 04/04 1530 | 120 | 400 | 300 | 100 | 13 | |
| 10 | 3 | 04/15 1400 | 04/18 1800 | 76.00 | 04/18 1522 | R | 40 -> 17 | -23 | 04/16 2350 | 100 | 670 | 320 | 350 | 13 | noisy |
| 11 | | 04/23 1400 | 04/25 0000 | 34.00 | 04/23 1729 | F | 50 -> 150 | 100 | 04/23 2133 | 330 | 470 | 320 | 150 | 19.2 | |
| | | | | | 04/23 2210 | / | 230 -> 270 | 40 | | | | | | | |
| 12 | 4 | 05/07 0600 | 05/08 1800 | 36.00 | 05/08 0922 | F | 50 -> 150 | 100 | 05/08 0952 | 210 | 690 | 480 | 210 | 13.5 | steps of T increase |
| 13 * | 5 | 05/15 1200 | 05/17 1800 | 54.00 | 05/15 1353 | F | 32 -> 90 | 58 | 05/16 0310 | 143 | 640 | 300 | 340 | 17 | 2 obviously different streams |
| 14 | 6 | 05/28 1400 | 05/30 1600 | 50.00 | 05/29 1515 | F | 110 -> 300 | 190 | 05/29 1525 | 320 | 730 | 340 | 390 | 20.6 | sharp interface |
| 15 | | 06/03 0600 | 06/04 0600 | 24.00 | | | | | 06/03 1127 | 120 | 520 | 395 | 125 | 13 | 3hrs data gap |
| 16 | 7 | 06/05 0000 | 06/07 1200 | 60.00 | | | | | 06/06 1920 | 125 | 660 | 350 | 310 | 14 | a trough |
| 17 * | | 06/14 1400 | 06/16 1000 | 44.00 | | | | | 06/15 0500 | 90 | 442 | 312 | 130 | 12 | following an ICME |
| 18 | 8 | 06/18 1800 | 06/20 1200 | 42.00 | | | | | 06/19 1300 | 180 | 520 | 300 | 220 | 16 | P plateau, no sharp increase of T |
| 19 * | 9 | 07/04 1800 | 07/06 1800 | 48.00 | 07/05 0352 | F | 55 -> 150 | 95 | 07/05 0417 | 200 | 670 | 400 | 270 | 14 | followed by an ICME |
| 20 * | 10 | 07/15 1200 | 07/17 0400 | 40.00 | 07/15 2040 | F | 75 -> 110 | 35 | 07/16 0457 | 340 | 640 | 300 | 340 | 22.5 | 2 obviously different streams |
| | | | | | 07/16 0020 | F | 90 -> 15 | -75 | | | | | | | |
| 21 | | 07/20 2000 | 07/22 0000 | 28.00 | | | | | 07/21 0510 | 163 | 500 | 335 | 165 | 15.5 | |
| 22 | 11 | 07/22 1200 | 07/23 2000 | 32.00 | 07/23 1302 | R | 120 -> 60 | -60 | 07/23 0307 | 240 | 740 | 360 | 380 | 16.6 | |
| 23 | | 08/05 2000 | 08/08 0400 | 56.00 | 08/06 0715 | F | 70 -> 180 | 110 | 08/06 0828 | 225 | 540 | 350 | 190 | 22 | |
| 24 | 12 | 08/22 0000 | 08/23 2200 | 46.00 | 08/22 0211 | F | 45 -> 75 | 30 | 08/22 1445 | 140 | 580 | 280 | 300 | 13.5 | |
| | | | | | 08/23 1025 | R | 80 -> 40 | -40 | | | | | | | |
| 25 | | 09/11 0200 | 09/13 0800 | 54.00 | | | | | 09/12 1552 | 80 | 510 | 330 | 180 | 9.5 | |
| 26 | | 09/17 1200 | 09/19 0800 | 44.00 | | | | | 09/18 1340 | 210 | 475 | 300 | 175 | 20 | |
| 27 | 13 | 10/06 1530 | 10/08 0000 | 32.50 | 10/06 1533 | / | 23 -> 46 | 23 | 10/07 1630 | 148 | 600 | 340 | 260 | 15 | ACE, a trough in P, 18 hrs data gap of Wind |
| 28 | 14 | 10/27 0600 | 10/30 0000 | 64.00 | | | | | 10/28 2100 | 95 | 630 | 350 | 280 | 12.5 | |
| 29 | 15 | 11/23 1000 | 11/24 0300 | 17.00 | | | | | 11/23 1630 | 150 | 520 | 310 | 210 | 16 | |
| 30 | | 12/10 1200 | 12/12 1200 | 48.00 | 12/11 1934 | F | 60 -> 120 | 60 | 12/11 2014 | 180 | 410 | 330 | 80 | 17.3 | ACE, 2 peaks of P |
| 31 | 16 | 12/15 1800 | 12/16 1100 | 17.00 | | | | | 12/16 0445 | 103 | 540 | 370 | 170 | 13 | ACE |
| 32 | 17 | 12/19 1200 | 12/21 0000 | 36.00 | | | | | 12/20 0000 | 80 | 500 | 340 | 160 | 11 | |
| 33 | 18 | 12/25 0200 | 12/26 0600 | 28.00 | 12/26 0414 | R | 110 -> 65 | -45 | 12/25 2000 | 220 | 540 | 320 | 220 | 22 | |

F/R shock: forward/reverse shock; ΔV: change in solar wind velocity during the event; *: hybrid event; /: not a shock.

**Table 2. Occurrence Rates of Shocks for SIRs**

| Year | | 1995 | 1996 | 1997 | 1998 | 1999 | 2000 | 2001 | 2002 | 2003 | 2004 | All |
|---|---|---|---|---|---|---|---|---|---|---|---|---|
| SIR # | | 36 | 34 | 36 | 33 | 36 | 32 | 33 | 41 | 44 | 40 | **365** |
| # of SIR with Shock(s) | | 17 | 6 | 9 | 13 | 13 | 6 | 9 | 10 | 8 | 4 | **95** |
| # with only Forward Shock | | 6 | 5 | 8 | 9 | 7 | 4 | 6 | 6 | 5 | 1 | **57** |
| # with only Reverse Shock | | 9 | 1 | 1 | 3 | 2 | 2 | 2 | 2 | 3 | 3 | **28** |
| # with a Pair of Forward-reverse Shock | | 2 | | | 1 | 4 | | | 1 | 2 | | **10** |
| of all SIRs | % with Shock(s) | 47.2 | 17.6 | 25.0 | 39.4 | 36.1 | 18.8 | 27.3 | 24.4 | 18.2 | 10.0 | 26.03 |
| | % with only Forward Shock | 16.7 | 14.7 | 22.2 | 27.3 | 19.4 | 12.5 | 18.2 | 14.6 | 11.4 | 2.5 | 15.62 |
| | % with only Reverse Shock | 25.0 | 2.9 | 2.8 | 9.1 | 5.6 | 6.3 | 6.1 | 4.9 | 6.8 | 7.5 | 7.67 |
| | % with a Pair of Forward-reverse Shock | 5.6 | | | 3.0 | 11.1 | | | 2.4 | 4.5 | | 2.74 |
| of SIRs with Shocks | % with only Forward Shock | 35.3 | 83.3 | 88.9 | 69.2 | 53.8 | 66.7 | 66.7 | 60.0 | 62.5 | 25.0 | 60.00 |
| | % with only Reverse Shock | 52.9 | 16.7 | 11.1 | 23.1 | 15.4 | 33.3 | 22.2 | 20.0 | 37.5 | 75.0 | 29.47 |
| | % with a Pair of Forward-reverse Shock | 11.8 | | | 7.7 | 30.8 | | | 10.0 | 25.0 | | 10.53 |

**Figure 4.** Occurrence Rates of SIRs with Shocks Relative to SIRs

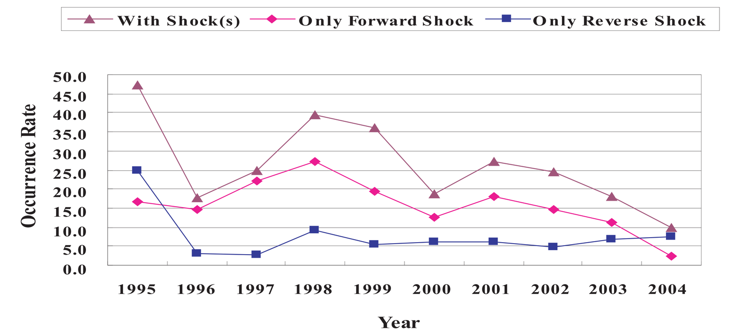


**Table 3. SIR Statistics**

| Year | <Duration> (δD) | <Rd=Dbefore/Dafter> (δRd) | <Pmax> (δPmax) | <Bmax> (δBmax) | < Rv=Vmax/Vmin > (δRv) | < ΔV > ( δΔV) |
|---|---|---|---|---|---|---|
| 1995 | 39.28 (3.28) | 1.06 (0.16) | 221.71 (20.20) | 17.15 (0.89) | 1.83 (0.06) | 270.74 (16.99) |
| 1996 | 36.41 (2.96) | 0.93 (0.12) | 132.85 (8.46) | 13.03 (0.47) | 1.55 (0.02) | 192.79 (9.66) |
| 1997 | 27.08 (1.84) | 1.28 (0.23) | 137.47 (8.07) | 12.96 (0.49) | 1.50 (0.03) | 163.24 (9.60) |
| 1998 | 43.62 (2.99) | 1.16 (0.16) | 172.61 (13.13) | 15.76 (0.64) | 1.70 (0.05) | 228.55 (15.09) |
| 1999 | 40.00 (3.09) | 1.04 (0.16) | 215.53 (21.60) | 17.44 (1.19) | 1.75 (0.06) | 254.78 (18.94) |
| 2000 | 33.71 (2.11) | 1.44 (0.23) | 219.27 (30.35) | 17.05 (1.14) | 1.68 (0.06) | 236.30 (16.76) |
| 2001 | 35.73 (3.10) | 1.02 (0.18) | 178.33 (18.54) | 15.77 (0.76) | 1.65 (0.04) | 217.94 (13.04) |
| 2002 | 36.26 (2.02) | 1.59 (0.34) | 230.86 (23.35) | 17.29 (0.96) | 1.70 (0.05) | 240.83 (17.09) |
| 2003 | 39.10 (3.03) | 0.98 (0.12) | 189.12 (19.17) | 16.60 (0.84) | 1.70 (0.05) | 263.44 (15.50) |
| 2004 | 47.07 (3.49) | 1.40 (0.25) | 141.41 (9.01) | 14.20 (0.67) | 1.70 (0.05) | 242.35 (18.08) |
| **All** | **37.96 (0.94)** | **1.19 (0.07)** | **177.11 (5.66)** | **15.50 (0.26)** | **1.67 (0.02)** | **232.50 (4.91)** |
| **Max** | **108.00** | **12.22** | **850** | **41** | **2.96** | **603** |
| **Min** | **7.00** | **0.02** | **52** | **7.2** | **0.72** | **61** |

**Figure 7.** Probability Distribution: Pmax and ΔV of SIRs (1995~2004)

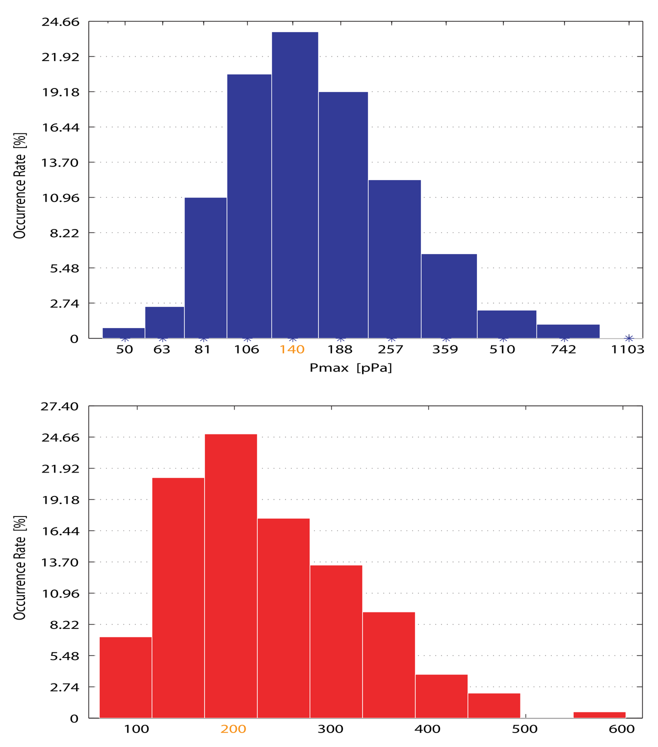


**Figure 8.** Probability Distribution: Pmax and ΔV of CIRs (1995~2004)

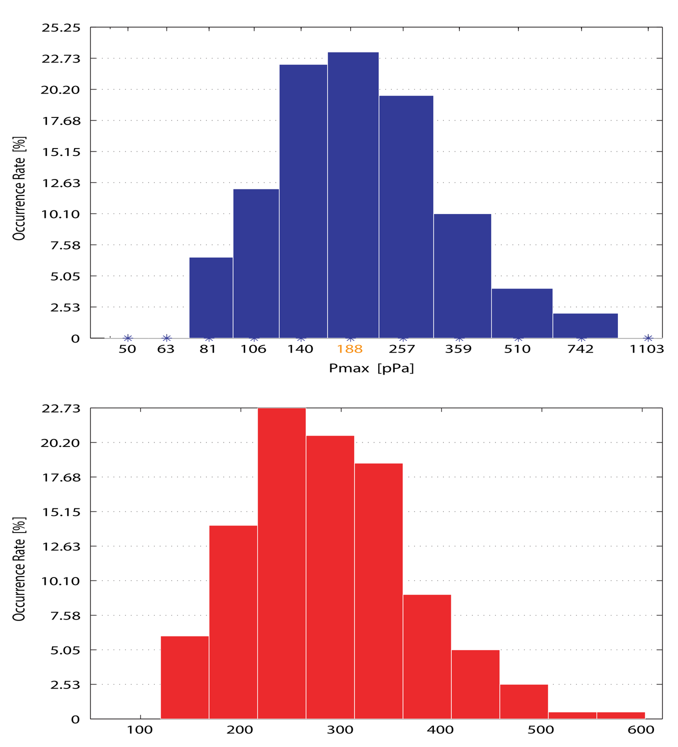


## Signatures in the Total Perpendicular Pressure (Ptpp)

Assuming a constant solar wind electron temperature, 130,000 K, and a constant 4% composition (by number) of alpha particles with a temperature 4 times that of the protons, we have calculated the total perpendicular pressure for the entire Wind (SWE and MFI) solar wind data set and ACE (SWEPAM and magnetometer) solar wind data set. Our criteria are mainly dependent on the behavior of Ptpp and are next most dependent on the solar wind speed (must be increasing). Other characteristics such as the compression of proton number density and magnetic field at the interface is approached, flow deflections and increased temperature at the interface give additional assurance of the identification. We show 2 interesting examples herein.

Figure 2 illustrates an SIR without shocks. The Ptpp profile is simple: an acceleration phase followed by a deceleration phase on an increasing speed profile. The components vary in a complex way. In the acceleration phase, the thermal speed of the protons is constant and the density of the protons rises; while there is a sharp density drop at the interface; and then the density and thermal speed both gradually decline in the deceleration phase.

Figure 3 gives one SIR with a Ptpp enhancement bounded by a pair of forward-reverse shocks. In the acceleration phase, the number density of protons are compressed and the thermal speed decreases while the Ptpp increases; while the deceleration phase has a declining temperature and density; the magnetic field without rotations mimics Ptpp.

## Occurrence Rate of SIRs and SIRs with Shocks during the Period 1995-2004

Based on 1995-2004 Wind and ACE solar wind data, we have identified 365 SIR events. Excluding data gaps and noisy data at both the two spacecraft, the annual average SIR event number is about 37. Table 1 presents a detailed list of the SIRs and CIRs for 1998, one of the 10 years for which lists have been made.

In the study, we define the boundary to be at the rapid jump of pressure if there is a shock; if not, we generally set the boundary based on the behavior of total pressure, like where the pressure structure emerges from and decays back to the ambient solar wind. We denote stream interface (SI) where the Ptpp reaches the peak during one SIR, ΔP as the change of the Ptpp across the discontinuity, Pmax, Bmax as the peaks of Ptpp and B, Rv as the ratio of Vmax to Vmin, ΔV as the change in the solar wind speed, $D_{before}$ as the duration between the start time and the stream interface, $D_{after}$ as the duration between the SI and end time, Rd as the ratio of $D_{before}$ to $D_{after}$ to imply the asymmetry in geometry relative to SI for each event.

For a discontinuity simply indicated by Ptpp, we examine the V, Np, Tp, B one by one, to verify if it is a forward or reverse shock. We find 95 SIRs are associated with shocks, taking 26% of the whole 365 SIRs. Some of such events are associated with more than one shock. Table 2 gives the yearly number and percentage of SIRs with shocks; with only forward shock(s) or only a reverse shock, or with a pair of forward-reverse shocks. In all, besides 10 events occurring with forward-reverse shock pair, among the 95 SIRs with shocks, 57 SIRs, i.e., 60% are associated with only forward shock; while among the 95 SIRs with shocks, 28 events, i.e., 29% occur with only reverse shock. The former is about twice larger than the latter. This is controversial because the models of SIRs suggest that the forward and reverse shocks formed at about the same time but at different distances from the Sun, with the reverse shocks forming closer to the sun than the forward shocks in SIRs, causing us to see more reverse shocks than forward shocks at the same observation spot in the interplanetary space.

In addition, Figure 4 illustrates the occurrence rates of SIRs with different types of shocks over the 10 years. For the solar cycle 23 starting from 1996, solar minimum, we find that the occurrence rates of SIRs with shocks and of SIRs with only forward shocks both have a declining trend. This may partly be attributed to the higher occurrence rate of SIRs on the declining phase of solar cycle. However, in 2004, there are more SIRs occurring with only reverse shocks.

Assuming the wave propagates in the direction perpendicular to the magnetic field, the fast magnetoacoustic wave speed is $(V_A^2 + C_S^2)^{1/2}$. The number density of protons is lower in the deceleration phase of fast stream (indicated by 2) than in the acceleration phase of slow stream (indicated by 1); while the plasma temperature $T_2$ is larger than $T_1$. So, the magnetoacoustic wave speed $Mcs_2$ is larger than $Mcs_1$. Therefore, for a same large change of velocity in the normal direction, it is easier to produce a Mach number larger than 1 in the acceleration of the slow stream. This can explain why we see more forward shocks than reverse shocks. Meanwhile, shocks happen when the interaction is strong so that some of such SIRs associated with shocks occur near ICMEs or other SIRs, in which the physical interaction is complex and difficult to model.

## Solar Cycle Variation of the Properties of SIRs

Table 3 addresses average Duration, Rd ($D_{before}$/ $D_{after}$), Pmax, Bmax, Rv (Vmax/Vmin), ΔV as well as their probable errors of the mean from 1995 to 2004. Figure 5 shows the annual statistics of the properties of SIRs. The first panel is the solar cycle variation of the occurrence rate of SIRs. During the declining phase of solar cycle 23, there are more SIRs than at other times, with a maximum occurrence of 44 events in 2003, the second maximum, 41 and 40. And the small occurrence, 32, 33 occur around solar activity maximum. So the the occurrence rate of SIRs is also affected by the variation of solar magnetic configuration during the period under study, although smaller compared to ICMEs. In addition, we find that the duration of SIRs is shorter in 1997, 2000, 2001, i.e., around solar minimum and solar maximum, and ΔV is larger over the declining phase of solar cycle.

Averaged over all these SIRs, the duration is 38.0±0.9 hr, where the uncertainty is the probable error of the mean; Rd is 1.19±0.07, indicating that the leading part before stream interface generally lasts longer than trailing part afterward, which can benefit the simulation work; Pmax is 177±6 pPa; Bmax is 15.5±0.3 nT; Rv is 1.67±0.02, and ΔV is 233±5 km/s.

Both the Pmax and Bmax are smaller than in ICMEs, indicating that the average strength of the interaction of SIRs with the ambient solar wind is after all weaker than the one of ICMEs. And the ΔV of SIRs is much larger than that of ICMEs, consistent with the SIR's role in the interaction of fast streams with slow streams.

As a complete study, we also illustrate the annual statistics of the same properties of CIRs in Figure 6, using the same format. The occurrence rate of CIRs has a similar solar cycle dependence. The Bmax is large around the solar maximum, and the Rd of CIRs varies more greatly than SIRs. As expected, the Pmax, Bmax, ΔV and Rv of CIRs are larger than of SIRs.

Figure 7, 8 show the probability distributions of Pmax, ΔV of SIRs and CIRs respectively. The Pmax of SIRs is distributed mostly around 140 pPa, although it can vary from 52 pPa up to 850 pPa. And the ΔV profile of SIRs has a similar distribution, centered on 200 km/s, with a variation in the range 61 ~ 603 km/s. Similarly, for CIRs, Pmax is centered on 188 pPa, and ΔV is distributed around 250 km/s.

## Conclusions

Total perpendicular pressure, Ptpp, can simplify the identification of different types of interactions. A peak with gradual slopes on its two sides is the identifying feature in the pressure of Stream Interaction Region (SIR). From 1995 to 2004, the occurrence rates of SIRs and CIRs both have somewhat solar cycle dependence. On average about 26% of SIRs are associated with shocks. In addition, the average peak pressure Pmax is 177±6 pPa, and the average ΔV is as large as 233±5 km/s. We look forward to the launch of STEREO. STEREO will add two more observation points on either side of the WIND/ACE pair, enabling stream interaction to be probed only a day or so apart, and determine how steady SIRs are. This will enable us to study the evolution of the shocks surrounding transient SIRs and to explore the stability of the shocks at SIRs.

## Acknowledgements

We have used the WIND plasma and magnetic field data throughout. We thank the MIT and Goddard plasma team (A.J. Lazarus and K. Ogilvie) and the magnetometer team (R.P. Lepping) for making these data available. We have supplemented this study with ACE data. We thank the PI of the plasma analyzer (D. McComas) and the magnetometer PI (C.W. Smith) for making these data publicly available, and also thank J. Steinberg and R. Skoug for giving us the access to ACE STEA electron pitch angle plots.